Inner-Sphere Self-Exchange Electron Transfer in Low-Spin Co(III)−Co(II) Couples. Rate Determinations from ^{1}H-NMR Line Broadening and a Simple Vibronic Model of the Reaction Coordinate

Carolyn L. Schwarz and John F. Endicott*

Department of Chemistry, Wayne State University, Detroit, Michigan 48202

Received March 2, 1995[⊗]

Inner-sphere electron transfer self-exchange rate constants have been determined using ^{1}H-NMR line broadening for several low-spin Co(III)−Co(II) couples of the type $Co(MCL)(OH_2)X^{2+}-Co(MCL)(OH_2)_2^{2+}$, where MCL = a tetraazamacrocycle coordinated equatorially and X = Cl, Br, or N_3. This work confirms previous inferences, based mostly on cross-reaction data, that (1) the inner-sphere rate constants are about 10^6 times larger than the equivalent outer-sphere rate constants and (2) variations of some of the inner-sphere rate constants (at least those with X = Cl) parallel differences in reactant and product molecular structure but (3) the inner-sphere rate constants are much less sensitive to structural variations than are the equivalent outer-sphere rate constants. The characteristically smaller inner-sphere nuclear reorganizational barrier can be attributed in part to correlation of the Co(III)−X^- stretch and the X^-−Co(II) compression, and this suggests that electron transfer occurs in concert with the motion of the bridging ligand. A simple vibronic model is proposed to accommodate this concerted motion of the bridging ligand and the very strong donor−acceptor coupling in these systems. This model suggests that the nuclear reorganizational parameters for inner-sphere cross-reactions will not be averages of those of the self-exchange reaction components if electron transfer is accompanied by large nuclear displacements and if the bridging ligand is comparable in mass to the donor and acceptor. Further implications of this model for strong vibronic coupling are the lack of Marcus-inverted region behavior and variations of inner-sphere self-exchange rate constants with the mass of the bridging ligand.

Introduction

One of the earliest classes of electron transfer reactions to be mechanistically characterized was that in which electron transfer was coupled to the transfer of a bridging ligand.[1−3] The classical "Taube reaction", eq 1,[1] is a particularly well-

$$Cr(OH_2)_6^{2+} + Co(NH_3)_5Cl^{2+} \xrightarrow{H_3O^+} Cr(OH_2)_5Cl^{2+} + Co(OH_2)_6^{2+} + 5NH_4^+ \quad (1)$$

characterized example of such an inner-sphere electron transfer pathway. Despite this extensive history, and in contrast to the attention given to and the successes of theoretical models of weakly coupled electron transfer systems,[2,4−14] there are still no widely accepted or well-established theoretical models of the inner-sphere pathway.[15] The two most obvious impediments to the evolution of such models are (a) the problem of treating very strong donor−acceptor coupling and (b) the problem of how one should approach the treatment of synergistic motions of the electron and the bridging ligand. It seems likely that the combination of these factors would invalidate the Born−Oppenheimer approximation which is usually a key premise of electron transfer theories[2,4−14] and which is the basis for the usual approach of treating separately the effects of nuclear reorganizational energies (λ_{DA}) and donor−acceptor electronic coupling (H_{DA}) on electron transfer rates. Failure of the Born−Oppenheimer approximation is expected to lead to more complex theoretical models.

In the absence of useful theoretical models, it seems appropriate that the key features of the inner-sphere reaction coordinate should be delineated by experimental studies. Some previous experimental studies have demonstrated that, while typical halide-bridged electron transfer reactions of Co(III)−Co(II)[1,16,17] or Cr(III)−Cr(II)[18] couples (couples with σ-donors

[⊗] Abstract published in *Advance ACS Abstracts,* August 1, 1995.

(1) (a) Taube, H.; Myers, H; Rich, R. L. *J. Am. Chem. Soc.* **1953**, *75*, 4118. (b) Taube, H. *Electron Transfer Reactions of Complex Ions in Solution*; Academic Press: New York, 1970.
(2) Cannon, R. D. *Electron Transfer Reactions*; Butterworths: Washington, DC, 1980.
(3) Haim, A. *Prog. Inorg. Chem.* **1983**, *30*, 273.
(4) (a) Marcus, R. A. *Annu. Rev. Phys. Chem.* **1964**, *15*, 155. (b) Marcus, R. A. *Rev. Mod. Phys.* **1993**, *65*, 599.
(5) Marcus, R. A.; Sutin, N. *Biochim. Biophys. Acta* **1985**, *811*, 265.
(6) Sutin, N. *Prog. Inorg. Chem.* **1983**, *30*, 441.
(7) Newton, M. D.; Sutin, N. *Annu. Rev. Phys. Chem.* **1984**, *35*, 437.
(8) Endicott, J. F. in *Encyclopedia of Inorganic Chemistry* Crabtree, R. H., King, R. B., Eds.; Wiley-Interscience: Sussex, England, 1994; Vol. 3, p 1081.
(9) Hush, N. S. In *Mechanistic Aspects of Inorganic Reactions*; Rorabacher, D. B., Endicott, J. F., Eds.; ACS Symposium Series 198; American Chemical Society: Washington, DC, 1982; Chapter 13, p 301.
(10) Mikkelsen, K. V.; Ratner, M. A. *Chem. Rev.* **1987**, *87*, 113.
(11) Newton, M. D. *Chem. Rev.* **1991**, *91*, 767.
(12) Electron Transfer in Biology and the Solid State. In *Inorganic Compounds with Unusual Properties*; Johnson, M. K., King, R. B., Kurtz, D. M., Kutal, C., Norton, M. L., Scott, R. A., Eds.; Advances in Chemistry Series 226; American Chemical Society: Washington, DC, 1990.
(13) *Photoinduced Electron Transfer, Part A. Conceptual Basis*; Fox, M. A., Channon, M., Eds.; Elsevier: New York, 1987.
(14) *Electron Transfer in Inorganic, Organic and Biological Systems*; Bolton, J. R., Mataga, N., McLendon, G., Eds.; Advances in Chemistry Series 228; American Chemical Society; Washington, DC, 1991.
(15) (a) Burdett[15b] has presented a treatment of the transition state of inner-sphere electron transfer systems which has many features in common with our treatment of electronic coupling in the transition state. (b) Burdett, J. K. *Inorg. Chem.* **1978**, *17*, 2537.
(16) (a) Durham, B.; Endicott, J. F.; Wong, C.-L.; Rillema, D. P. *J. Am. Chem. Soc.* **1979**, *101*, 847. (b) Kumar, K.; Rotzinger, F. P.; Endicott, J. F. *J. Am. Chem. Soc.* **1983**, *105*, 7064.
(17) Rillema, D. P.; Patel, R. C.; Endicott, J. F. *J. Am. Chem. Soc.* **1972**, *94*, 394.

0020-1669/95/1334-4572$09.00/0

and σ-acceptors) are 10^6-10^7 times faster than the equivalent outer-sphere electron transfer reactions,[1-3,19] many of these reaction rates are still strongly dependent on parameters such as the free energy of reaction and apparent nuclear reorganizational energies.[16,17,19] These parameters are typical components of the Franck−Condon (i.e., nuclear coordinate dependent) factors of the common treatments of weakly coupled, outer-sphere electron transfer reactions.[2,3-14] Other studies have indicated a strong dependence of such inner-sphere rates on electronic factors.[16,19,20] Thus, it appears that very similar factors contribute to inner- and outer-sphere electron transfer processes, but it is not clear whether the nuclear and electronic factors can be treated as separable in the inner-sphere processes.

In our earlier studies we developed a series of low-spin Co(III)−Co(II) couples containing equatorial tetraazamacrocyclic ligands.[16,21] The different macrocyclic ligands resulted in different Franck−Condon factors for electron exchange,[21] and it is this feature which has enabled us to use these couples to probe the details of inner-sphere reaction pathways. A puzzling feature of these earlier studies of the low-spin Co(III)−Co(II) couples was the inference that the apparent nuclear reorganizational parameter, λ(IS), for the inner-sphere pathway was approximately half that of the equivalent outer-sphere electron transfer process.[16a] It seems possible that this behavior could have its origin in the combined nuclear and electronic motion characteristic of these systems, but there has been no theoretical justification for such an inference. Furthermore, this inferred relationship, $\lambda(IS) \sim \lambda(OS)/2$, was based on a fit of cross-reaction data to a Marcus formalism[4-8] for weakly coupled electron transfer systems, so that the physical significance of the inferred values of λ(IS) was not clear.

The studies described in this report were undertaken in part to determine whether the apparent values of λ(IS) inferred from cross-reactions are consistent with those obtained from self-exchange reactions, and we wished to explore the possibility of finding a simple model of the reaction pathway which would be compatible with the $\lambda(IS) \sim \lambda(OS)/2$ relationship. In this regard, we recently found that a Jahn−Teller-like, vibronic approach is useful for many aspects of the behavior of very strongly coupled, bridged, π-type (Ru−L−Ru, where L is a π-conjugated ligand) donor−acceptor systems.[22] The halide-bridged, σ-type donor−acceptor systems are intrinsically simpler (three rather than four coupled states), and we develop a vibronic approach to the inner-sphere reaction coordinate in this report.

Experimental Section

Literature procedures were used to prepare *trans* complexes of the types: $[Co(MCL)(OH_2)_2]ClO_4)_3$,[17-23] $[Co(MCL)(OH_2)_2](ClO_4)_2$,[23-25] $[Co(MCL)X_2]ClO_4$ (X = Cl,[23,26-28] Br,[23,26-30] or N_3[30-32]), $[Co(MCL)(N_3)X]ClO_4$ (X = Cl[31,32] or Br[29]), or $[Co(MCL)OH_2)X](ClO_4)_2$ (X = Cl,[30,32] Br,[29,31] or N_3[31,32]); MCL = Me_4[14]tetraeneN$_4$, Me_2pyo[14]trieneN$_4$, Me_2[14]1,11-dien-13-oneN$_4$, or Me_6[14]4,11-dieneN$_4$[33] (see Figure 1). **Warning: These perchlorate salts are potentially explosive and should be handled with great caution.**

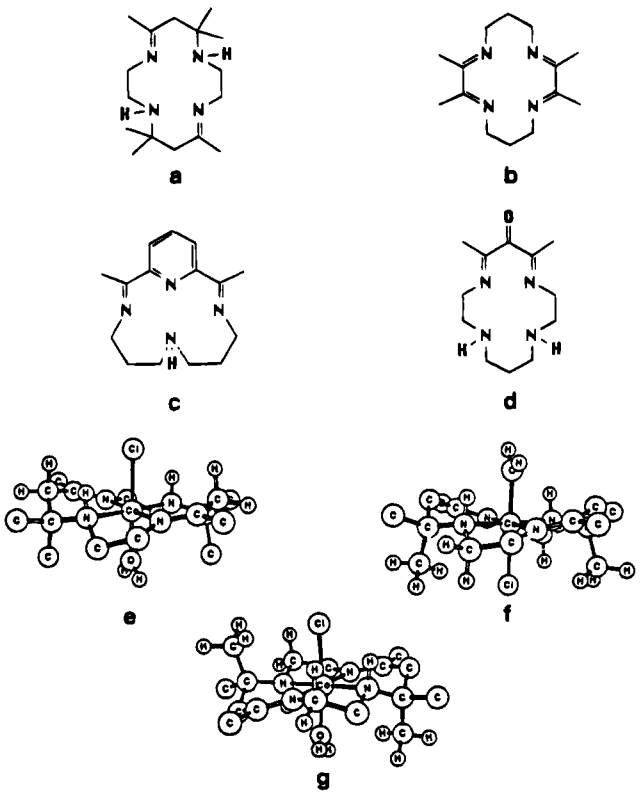

Figure 1. Skeletal and stereochemical structures of macrocyclic ligands and complexes: (a) Me_6[14]dieneN$_4$; (b) Me_4[14]tetraeneN$_4$; (c) Me_2pyo[14]trieneN$_4$; (d) Me_2[14]1,11-dien-13-oneN$_4$; (e) [primary]-*rac*-Co(Me_6[14]dieneN$_4$)$(OH_2)Cl^{2+}$; (f) [secondary]-*rac*-Co(Me_6[14]dieneN$_4$)$(OH_2)Cl^{2+}$; (g) *meso*-Co(Me_6[14]dieneN$_4$)$(OH_2)Cl^{2+}$. Previous work[39] has shown complex e to be the most stable Co(Me_6[14]dieneN$_4$)$(OH_2)Cl^{2+}$ isomer, while complex g has the ligand conformation of the most stable isomer of Co(Me_6[14]dieneN$_4$)$(OH_2)_2^{2+}$.[38,53]

[*trans*-Co(Me_4[14]tetraeneN$_4$)(OH_2)Cl](ClO$_4)_2$. This complex was prepared in a manner analogous to that reported for [*trans*-Co(Me_4[14]tetraeneN$_4$)(OH_2)Br]$(ClO_4)_2$.[31] Perchloric acid (25 mL, 70%) was added to a hot suspension of $[Co(Me_4[14]tetraeneN_4)(N_3)(Cl)]ClO_4$ (0.83 g) in absolute ethanol (50 mL). The solution was heated until a bluish-green color was observed. The solution was filtered to remove the $[Co(Me_4[14]tetraeneN_4)(Cl)_2]ClO_4$ which was formed as a side product. A mixture of ethanol/acetone (100 mL; 2:1, v/v) was added to the filtrate followed by excess diethyl ether to precipitate a light green solid. The solid was filtered off, washed with diethyl ether, and then dried under vacuum at 65 °C.

[*trans*-Co(*rac*-Me_6[14]4,11-dieneN$_4$)$(OH_2)_2$](ClO$_4)_2$. This complex was prepared from [*trans*-Co(*rac*-Me_6[14]4,11-dieneN$_4$)(OH_2)X]$(ClO_4)_2$ (X = Cl or Br) dissolved and deaerated in a minimum amount of hot 1.0 M $HClO_4$. A chromous perchlorate solution in 1 M $HClO_4$ was added to the solution under N_2. A yellowish color was seen as soon

(18) (a) Ball, D. L.; King, E. L. *J. Am. Chem. Soc.* **1958**, *80*, 1091. (b) James, R. V.; King, E. L. *Inorg. Chem.* **1970**, *9*, 1301. (c) Snellgrove, R.; King, E. L. *J. Am. Chem. Soc.* **1962**, *84*, 4609.
(19) Endicott, J. F.; Kumar, K.; Ramasami, T.; Rotzinger, F. P. *Prog. Inrog. Chem.* **1983**, *30*, 141.
(20) Rotzinger, F. P.; Kumar, K.; Endicott, J. F. *Inorg. Chem.* **1982**, *21*, 4111.
(21) Endicott, J. F.; Durham, B.; Glick, M. D.; Anderson, T. J.; Kuszaj, W. G.; Schmonsees, W. G.; Balakrishnan, K. R. *J. Am. Chem. Soc.* **1981**, *103*, 1431.
(22) (a) Watzky, M. A.; Endicott, J. F.; Buranda, T. *J. Phys. Chem.*, submitted for publication. (b) Watzky, M. A. Ph.D. Dissertation, Wayne State University, 1994.
(23) Durham, B. Ph.D. Dissertation, Wayne State University, 1977.
(24) Rillema, D. P.; Endicott, J. F. *J. Am. Chem. Soc.* **1972**, *94*, 8711.
(25) Rillema, D. P.; Endicott, J. F.; Papaconstaninou, E. *Inorg. Chem.* **1971**, *10*, 1739.
(26) Jackels, S. C.; Farney, K.; Barefield, E. K.; Rose, N. J.; Busch, D. H. *Inorg. Chem.* **1972**, *11*, 2893.
(27) (a) Long, K. M.; Busch, D. H. *J. Coord. Chem.* **1974**, *4*, 113. (b) Long, K. M.; Busch, D. H. *Inorg. Chem.* **1970**, *9*, 505.
(28) Switzer, J. A. Ph.D. Dissertation, Wayne State University, 1979.
(29) Poon, C.-K.; Lee, W. K. J. *Chem. Soc., Dalton Trans.* **1974**, 2423.
(30) Sadasivan, N.; Kernohan, J. A.; Endicott, J. F. *Inorg. Chem.* **1967**, *6*, 770.
(31) Poon, C.-K.; Wong, C.-L. *J. Chem. Soc., Dalton Trans.* **1976**, 966.
(32) Wong, C.-L. Ph.D. Dissertation, University of Hong Kong, 1976.
(33) Abbreviations of ligand names: Me_4[14]tetraeneN$_4$ = 2,3,9,10-tetramethyl-1,4,8,11-tetraazacyclotetradeca-1,3,8,10-tetraene; Me_6[14]4,11-dieneN$_4$ = 5,7,7,12,14,14-hexamethyl-1,4,8,11-tetraazacyclotetradeca-4,11-diene; Me_2[14]-1,11-dien-13-oneN$_4$ = 12,14-dimethyl-1,4,8,11-tetraazacyclotetradeca-1,11-dien-13-one; Me_2pyo[14]trieneN$_4$ = 2,12-dimethyl-3,7,11,17-tetraazabicyclo[11.3.1]septadeca-1(17)2,-11,13,15-pentaene.

Table 1. Elemental Analysis of Selected Complexes

compound	% found (% theoretical) C	H	N	C/N
$[Co(Me_6[14]4,11\text{-dieneN}_4)(OH_2)_2](ClO_4)_2$	33.45 (33.50)	6.15 (6.30)	9.81 (9.80)	3.41 (3.42)
$[Co(Me_6[14]4,11\text{-dieneN}_4)(OH_2)Br](ClO_4)_2$	30.45 (30.20)	5.71 (5.70)	8.90 (8.81)	3.42 (3.43)
$[Co(Me_6[14]4,11\text{-dieneN}_4)(OH_2)Cl](ClO_4)_2 \cdot 2.5\ H_2O$	30.12 (30.18)	6.08 (6.17)	8.80 (8.80)	3.42 (3.43)
$[Co(meso\text{-}Me_6[14]4,11\text{-dieneN}_4)Cl_2](ClO_4) \cdot 1.5\ H_2O$	35.53 (35.80)	6.41 (6.57)	10.42 (10.44)	3.41 (3.43)
$[Co(Me_6[14]4,11\text{-dieneN}_4)Cl_2]ClO_4$	37.69 (37.70)	6.42 (6.33)	10.95 (11.00)	3.44 (3.43)
$[Co(Me_4[14]\text{tetraeneN}_4)(OH_2)_2](ClO_4)_2$	31.51 (31.00)	5.32 (5.20)	9.96 (10.30)	3.16 (3.01)
$[Co(Me_2[14]1,11\text{-dien-13-oneN}_4)(OH_2)N_3](ClO_4)_2$	25.73 (25.91)	4.39 (4.35)	18.21 (17.63)	1.41 (1.47)
$[Co(Me_2[14]1,11\text{-dien-13-oneN}_4)(OH_2)_2](ClO_4)_2 \cdot 0.5H_2O \cdot 0.5HClO_4$	24.08 (24.37)	4.43 (4.69)	9.76 (9.47)	2.47 (2.57)
$[Co(Me_2\text{pyo}[14]\text{trieneN}_4(OH_2)_2]\ (ClO_4)_2 \cdot H_2O$	31.97 (31.59)	4.23 (4.95)	9.65 (9.82)	3.31 (3.22)

as the Cr^{2+} was added. The solution was cooled immediately, and a yellow solid began to form. $NaClO_4$ solid can be added to aid in precipitation of the product if it has not occurred within a few minutes of cooling. The solid was filtered off, washed with cold 1.0 M $HClO_4$ and diethyl ether, and dried under vacuum at 50 °C for a minimum of 2 h. The solid will decompose if not completely dry.

Other Complexes. The *trans*-$Co(Me_2\text{pyo}[14]\text{trieneN}_4)(OH_2)X^{2+}$ complexes (X = Cl and Br) were not isolated as solids but were prepared in D_2O solution by reaction of $Co(Me_2\text{pyo}[14]\text{trieneN}_4)(OH_2)_2^{3+}$ with NaBr and NaCl, respectively. The extent of the substitution of the halide in the complex was monitored by NMR at 25 °C. The same approach was used for the *trans*-$Co(Me_2[14],11\text{-dien-13-oneN}_4)(OH_2)X^{2+}$ (X = Cl, Br) complexes.

Elemental analyses were performed by Midwest Microlab, Indianapolis, IN, or the Central Instrumentation Facility, Wayne State University, Detroit, MI. Samples were analyzed for C, H, and N. The results are summarized in Table 1.

Gaseous nitrogen streams were deoxygenated using a De-Ox catalyst purchased from Alfa Products and reduced with stream of H_2 (5%) in Ar at 110−150 °C.

Solutions of Cr^{2+} were prepared from $Cr(ClO_4)_3 \cdot 6H_2O$, e.g., 9.16 g dissolved in 100 mL of 1.0 M $HClO_4$. Deoxygenated nitrogen was bubbled through the Cr^{3+} solution for 1 h, and then the Zn amalgam was added. Nitrogen was allowed to pass through the solution overnight.

Solutions were prepared with D_2O (98 atom % purchased from Aldrich Chemical Co.) or H_2O distilled in a Corning Mega-Pure still. The water was pretreated with a Corning 3508-A Ultrahigh Purity Demineralizer.

Reactant solutions were prepared under a deoxygenated nitrogen atmosphere, and they were mixed and transferred with Teflon tubing. For light-sensitive materials, samples were prepared and transferred to instruments under low light.

Proton-NMR samples prepared in D_2O contained TMAP (tetramethylammonium perchlorate) as a standard and internal reference. Data was collected from 5 to 40 °C at 5 °C intervals. With normal 1 pulse parameters, the number of accumulations depended on the concentration of the diamagnetic species in solution. NMR peaks were analyzed for peak width and peak position. Rate constants for the pseudo-first-order reactions were determined from linear regression analysis of plots of $\nu_{1/2}$ vs the concentration of the paramagnetic species.

Instrumental Techniques. The ^{1}H-NMR spectra were determined on a Nicolet NT-300 spectrometer equipped with a Nicolet 1280 computer and a variable-temperature unit which used either N_2 or air. Some spectra were also recorded with a General Electric QE-300 or GN-300 spectrometer. Data collected on the NT-300 were stored on a removable hard disk data cartridge. Deconvolution and calculation of full width at half-height and areas under each peak were carried out using the CAP (Curve Analysis Program).

Visible and ultraviolet spectra were determined using a Cary 14 spectrophotometer and either 1.0 or 10.0 cm quartz cells.

Infrared spectra were recorded on a Nicolet 20DX Fourier transform spectrometer or on a Perkin-Elmer 283B double-beam infrared spectrometer using potassium bromide pellets.

Kinetic Techniques. The self-exchange electron transfer rate constants were determined from NMR line broadening for a series of $Co^{III,II}$ macrocycles. Most of the Co^{III} and Co^{II} complexes used were prepared as solids as described above. The NMR samples were prepared under nitrogen by dissolving known quantities of the complexes in dearated D_2O solution with transfer direct to an NMR tube. Solution conditions varied depending on the complex. NMR spectra were taken at eight temperatures from 5 to 40 °C in 5 °C increments. The instrument was shimmed at each temperature, although for this small temperature range only small adjustments were needed. Data were collected for standard samples, those which contained no paramagnetic species, and reaction samples which contained the paramagnetic species in varying concentrations. The data were saved on disk, and the workup was performed on an entire set at one time to minimize errors. Line widths were calculated by a Lorentzian fit procedure or a program, CAP (Curve Analysis Program), which deconvolutes overlapping peaks and calculates peak area, position, and line width. The line shape eq was used in the form

$$Y(i) = Y(0)\left(\frac{1}{1 + 4\left(\frac{x(0) - x(i)}{W}\right)^2}\right)$$

where the Gaussian correction has been neglected, $Y(0)$ is proportional to the entered intensity, W is the width at half-height, and $x(0)$ is the entered position. Values for height, width, and position were varied until the smallest rms values were obtained. In this work we used methyl singlets, and the only peaks deconvoluted arose from small amounts of $Co(MCL)(H_2O)_2^{3+}$ and $Co(MCL)(X)_2^+$ (X = Cl, Br, N_3) which were inevitably present in the reaction mixtures. Values of $\Delta\nu_{1/2}$ were based on the CAP fit.

Samples were run with tetramethylammonium perchlorate (TMAP) added as a reference and standard. Since NaTSP·H_2O could not be added as a reference due to reference peaks in the sample area of the spectrum, TMAP was useful in serving both functions. The reference frequency value was determined by setting the HDO peak at 4.80 ppm in the standard run at 25 °C. This reference value was then used in all runs, including those with the paramagnetic species present. The line widths for the standard were tabulated against temperature. It was important to determine if the presence of Co^{II} in solution at these concentrations had any effect on the line width. A sample of $[Co(Me_4[14]\text{tetraeneN}_4)(CN)_2]ClO_4$ with TMAP was used to explore this effect. It was not expected that electron transfer would be observed for this complex. Temperature studies were run with and without $Co(Me_4[14]\text{tetraeneN}_4)(OH_2)_2^{2+}$ present. We observed that the line widths

Table 2. Self-Exchange Electron Transfer Rate Constants Determined by ^{1}H-NMR Line Broadening for Co(MCL)$(OH_2)X^{2+}$/Co(MCL)$(OH_2)_2^{2+}$ Reactions

MCL	k_{exch},[a] M^{-1} s^{-1}			k_{exch}',[b] M^{-1} s^{-1}
	X = N_3	X = Cl^-	X = Br	
Me_6[14]4,11-dieneN$_4$	$\geq 8.9 \times 10^2$ [c]	$\geq 4 \times 10^2$ [c,e] 2×10^4 [d,e]	$\geq 4 \times 10^2$ [c,i]	4.5×10^{-5}
Me_4[14]tetraeneN$_4$	$(2.3 \pm 0.5) \times 10^5$	$(4.4 \pm 0.5) \times 10^5$ [f]		5×10^{-2}
Me_2pyo[14]trieneN$_4$	$(3.0 \pm 0.4) \times 10^5$	2×10^5 [g]	$\approx 1.3 \times 10^6$ [j]	9.3×10^{-2}
Me_2[14]1,11-dien-13-oneN$_4$	$(4.0 \pm 0.4) \times 10^5$	$(1.1 \pm 0.1) \times 10^4$ [h]		4.4×10^{-3}

[a] For inner-sphere reactions; 0.1 M HTFMS and 0.9 M NaTFMS, except an indicated. [b] For outer-sphere, Co(MCL)$(OH_2)_2^{3+,2+}$ reactions; ref 21. [c] *meso* isomer of Co(II). [d] *rac* isomer of Co(II). [e] 1.0 M HTFMS and 0.1 M NaCl. [f] 0.1 M HTFMS and 1.0 M NaCl. [g] $[Co^{3+}] = 6.7 \times 10^{-1}$ M, $[Co^{3+}]_{tot} = 9.98 \times 10^{-3}$ M, $[Co^{2+}] = 9.0 \times 10^{-4}-7.2 \times 10^{-5}$ M, $[Cl^-] = 1.78 \times 10^{-2}$ M. [h] $[Co^{3+}] = 2.9 \times 10^{-3}$ M, $[Co^{3+}]_{tot} = 1.29 \times 10^{-2}$ M, $[Co^{2+}] = 7.5 \times 10^{-4}-8.4 \times 10^{-5}$ M, $[Cl^-] = 2.91 \times 10^{-3}$M. [i] 1.0 M HTFMS. [j] 0.1 M HTFMS.

of the methyls of the cyanide complex or the TMAP methyls were broadened less than 1 Hz by the paramagnetic species for the concentrations used. This experiment also showed that the methyl line widths of the complex and those of TMAP behaved in similar ways so TMAP could be used to monitor paramagnetic line broadening in subsequent experiments.

The Co^{III}(MCL) peaks broadened markedly in the presence of Co^{II}(MCL) for the electron transfer systems. The self-exchange rate constants were calculated from a plot of corrected line widths $\Delta\nu_{1/2}$ (experimental line width minus standard line width) vs $[Co^{II}]$. The slopes of such plots equal k_{exch}/π in the limit of slow exchange, eq 2;[34-37] the peak maxima shifted very little with changes of [(Co(II)]

$$k = \frac{\Delta\nu_{1/2}(\text{obsd}) - \Delta\nu_{1/2}(\text{diamag})}{[P]} \qquad (2)$$

(e.g., see Figure 2; details of $\Delta\nu_{1/2}$ and peak maxima may be found elsewhere[38a]).

Results

The experimental values determined for the self-exchange rate constants of several inner-sphere electron transfer reactions are summarized in Table 2.

The azide complexes were studied in 0.1 M HFTMS and 0.9 M NaTFMS for a total ionic strength of 1.0 M. Of the four azide complexes studied, only for Co(Me_6[14]4,11-dieneN$_4$)$(N_3)(H_2O)^{2+}$ were reactions complicated by the presence of peaks due to a significant distribution of axially substituted species. The most intense methyl resonance for the reactant mixture was used to calculate the rate constant. A typical determination is illustrated in Figure 2.

The chloride and bromide complexes introduced other complications. The Co(Me_6[14]4,11-dieneN$_4$)$(Cl)(OH_2)^{2+}$ and Co(Me_6[14]4,11-dieneN$_4$)$(Br)(OH_2)^{2+}$ complexes could be prepared easily from literature procedures; however, the chloro aquo complex disproportionated fairly quickly under the conditions used in the azide reactions.[38] The Co(Me_6[14]4,11-dieneN$_4$)$(Br)(OH_2)^{2+}$ complex did yield a marginally measurable value. The Co(Me_6[14]4,11-dieneN$_4(OH_2)_2^{2+}$ complex was not very soluble under the solution conditions used for the azide complexes, but the slower reactions required relatively large Co(II) concentrations, so the reactions were run in 1.0 M HTFMS.

"Self-exchange" studies of Co(*rac*-Me_6[14]4,11-dieneN$_4$)$(Cl)(OH_2)^{2+}$ were performed with both the *meso* and *rac* isomers

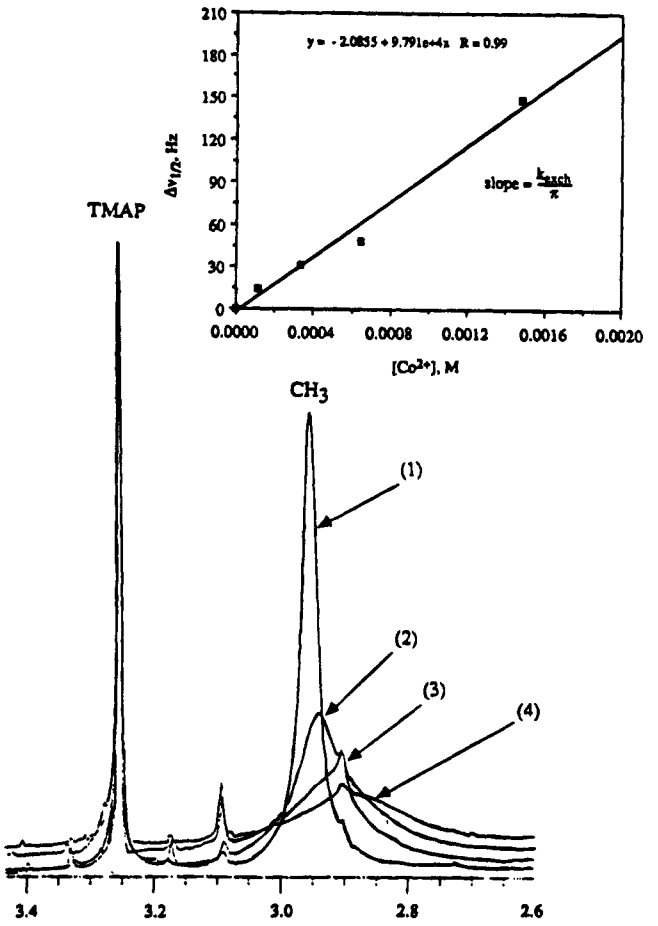

Figure 2. Line broadening due to self-exchange electron transfer illustrated by. NMR of Co(Me_4[14]tetraeneN$_4$)$(N_3)(H_2O)^{2+}$ with added Co(Me_4[14]tetraeneN$_4$)$(H_2O)^{2+}$. Reaction run at 25 °C in 0.1 M HTFMS/0.9 M NaTFMS/D_2O). $[Co^{2+}]$: (1) 0.00 M; (2) 1.3×10^{-4} M; (3) 3.3×10^{-4} M; (4) 6.5×10^{-4} M. The insert is a plot of line width vs $[Co^{2+}]$ for reactions with Co(Me_4[14]tetraeneN$_4$)$(N_3)(H_2O)^{2+}$ with Co(Me_4[14]tetraeneN$_4$)$(H_2O)^{2+}$. Line widths have been corrected for contact broadening by referencing to $N(CH_3)_4^+$ (<10% of total at any $[Co^{2+}]$).

of the Co(II) complex. The reactions were run in 1.0 M HTFMS and 0.1 M NaCl with TMAP at 25 °C. The reactant concentrations of these solutions were adjusted so that [Co(III)] and [Co(II)] would be 1.5×10^{-3} and 1.7×10^{-3} M, respectively. In the reaction with the *meso* isomer however the actual concentration of the Co^{II}(MCL) complex was smaller than this because the initial spectrum showed small extraneous peaks attributable to the decomposition of the Co(II) complex. A relatively small limiting value for the cross-reaction rate constant, based on these considerations and the line broadening observed, is 4×10^2 M^{-1} s^{-1}. Reactions with the pure racemic isomer of the Co(II) complex were also examined. Only the data points for

(34) Pearson, R. G.; Palmer, J.; Anderson, M. M.; Allred, A. L. Z. *Elektrochem.* **1960**, *64*, 110.
(35) Dietrich, M. W.; Wahl, A. C. *J. Chem. Phys.* **1963**, *38*, 1591.
(36) Canters, G. W.; Hill, H. A. O.; Kitchen, N. A. *Magn. Reson.* **1984**, *57*, 1.
(37) Goodwin, J. A.; Stanbury, D. M.; Wilson, L. J.; Eigenbrot, C. W.; Scheidt, W. R. *J. Am. Chem. Soc.* **1987**, *109*, 2979.
(38) (a) Schwarz, C. L. Ph.D. Dissertation, Wayne State University, 1988. (b) Schwarz, C. L.; Endicott, J. F. *Inorg. Chem.* **1989**, *28*, 4011.

Table 3. Equilibrium Constants and Conditions for the Anation Reactions $Co(MCL)(OH_2)_2^{2+} + X \rightarrow Co(MCL)(OH_2)X^{2+}$ at 25 °C

MCL	X	conditions	K_{eq}, M[a]
Me_2[14]4,11-dien-13-oneN_4	Cl	D_2O; 0.01 M NaCl; no TMAP	135
	Cl	D_2O; 0.0069 M NaCl; 0.002 M TMAP	120
	Br	D_2O; 0.0049 M NaBr; no TMAP	113
Me_2pyo[14]trieneN$_4$	Cl	D_2O; 0.0210 M NaCl; 0.0029 M TMAP	104

[a] Estimated ±15% uncertainty.

Table 4. Ratios of Inner-Sphere to Outer-Sphere Reaction Rate Constants (k_{IS}/k_{OS}) for Several Systems: $MX^{2+} + {}^*M^{2+} \rightleftharpoons M^{2+} + {}^*MX^{2+}$

bridging ligand X	M = Co(MCL)(OH$_2$)[a] MCL = Me_4[14]tetraeneN$_4$	MCL = Me_2pyo[14]trieneN$_4$	MCL = Me_2[14]1,11diene$_4$-13-oneN$_4$	M = Cr[b]
F				2.5×10^3
Cl	8.8×10^6	2.5×10^6	2.5×10^6	2.4×10^4
Br		$\geq 1.4 \times 10^7$ [b] ($\sim 8 \times 10^7$)[c]		$> 6 \times 10^7$
N_3	6×10^6	3.7×10^6	90×10^6	6.1×10^6

[a] k_{IS} for this study; k_{OS} from ref 20 (see Table 2); 1 M ionic strength. [b] k_{IS} from refs 17; $k_{OS} \sim 10^{-6}$ M^{-1} s^{-1}.[2,18] [c] For k_{IS} measured in 0.1 M ionic strength. [d] For k_{IS} estimated at 1 M ionic strength.

which the Co(II) concentration is lower than that of Co(III) were used to calculate the rate because there was evidence for decomposition at higher concentrations. The reactions were run using the same conditions as for the *meso* isomer; the self-exchange rate constant was calculated to be 2×10^4 M^{-1} s^{-1}.

The $Co(Me_4[14]tetraeneN_4)(OH_2)Cl^{2+}$ complex could be isolated as a perchlorate salt, but it aquated in solution. The electron transfer reactions were run in 1.0 M NaCl and 0.1 M HTFMS to suppress this reaction.

The $Co(Me_2[14]1,11\text{-dien-}13\text{-one}N_4)(OH_2)X^{2+}$ and $Co(Me_2\text{-pyo}[14]trieneN_4)(OH_2)X^{2+}$ complexes, where X = Cl or Br, could not be isolated as solids, nor could they be prepared in solution by dissolving $Co(MCL)X_2^+$, where X = Cl^- or Br^-, in strong acid. These species were prepared by addtion of Cl^- or Br^- to the diaquo species. Equilibrium concentrations of species were then measured on the basis of their NMR spectra. Table 3 gives the conditions and formation constants for these complexes.

Only the $Co(MCL)(H_2O)N_3^{2+}$ complexes were sufficiently stable with respect to disproportionation that we could examine the effects of temperature on k_{exch}. Of these, the complexes with MCL = Me_4[14]tetraeneN$_4$ and pyoMe_2[14]trieneN$_4$ exhibited only very shallow temperature dependencies (apparent $\Delta H^{\ddagger} \leq 2$ kJ mol^{-1}) which were not significantly outside reasonable error limits (Table 2). On the other hand, we found an 8-fold increase in k_{exch} between +5 and 40 °C for the complex with MCL = Me_2[14]1,11-dien-13-oneN$_4$ (apparent $\Delta H^{\ddagger} = 4.2$ kJ mol^{-1}, $\Delta S^{\ddagger} = 12$ J K^{-1} mol^{-1}).

Discussion

The class of inner-sphere self-exchange reactions examined in this study are conceptually very simple: (a) the macrocyclic ligands restrict substitutional processes to the axial coordination sites; (b) the electron being exchanged is in an axial orbital ($\sim d_{z^2}$) of the cobalt(II) partner; (c) the donor, the acceptor, and the bridging ligand orbitals (at least in the case of the halide bridging ligands) all have σ symmetry with respect to the M−X−M′ axis. In such a situation one expects that the coupling through the M−X−M′ network will be very strong and reasonably well-approximated by a 3-center bonding interaction.[16b,19,39] Qualitatively, a transition state 3-center bonding interaction would result in a corresponding decrease in the activation barrier, relative to that observed in the absence of such strong coupling (as in the outer-sphere analog). If this were the only factor of importance, then the much larger inner-sphere than outer-sphere rate constants in these systems would be attributed to bridging ligand dependent transition state 3-center bonding interactions which run over the range 35−50 kJ mol^{-1}. That such three-center bonding interactions are not the only factor influencing inner-sphere reaction patterns has been demonstrated by the free energy dependence and the apparent reorganizational energy dependence of cross-reaction rates[16,17] and by the variations in inner-sphere self-exchange rate constants found in this study. Thus, the macrocyclic ligand induced structural variations which lead to a 2000-fold variation of outer-sphere self-exchange electron transfer rate constant for the *trans*-$Co(MCL)(OH_2)_2^{3+,2+}$ couples do seem to have weaker parallels in the variations of k_{exch} for the inner-sphere reactions. Detailed features of the observed inner-sphere self-exchange reaction pathways are discussed below.

The attenuated sensitivity of the inner-sphere self-exchange rate constants to variations in macrocyclic ligand induced structural changes (relative to rate constants for the analogous outer-sphere reactions)[21] is consistent with the earlier inference that $\lambda_{DA}(IS) \ll \lambda_{DA}(OS)$. Before we can consider how this attenuation might come about, it is necessary to define some key features of the inner-sphere reaction pathway. An inner-sphere self-exchange reaction can be represented in terms of a sequence of steps which may, in principle, be discrete (the asterisk is an arbitrary label used to distinguish reaction partners) as in eqs 3−6. The quantities {A,B} represent "collision complexes" or "ion pairs". The lifetime (k_w^{-1}) of coordinated water in the low-spin cobalt(II) complexes has been estimated to be 10^{-8}−10^{-9} s.[16,39] This is probably comparable to, or

(39) (a) Endicott, J. F.; Wong, C.-L.; Ciskowski, J. M.; Balakrishnan, K. P. *J. Am. Chem. Soc.* **1980**, *102*, 2100. (b) Endicott, J. F.; Balakrishnan, K. P.; Wong, C.-L. *J. Am. Chem. Soc.* **1980**, *102*, 5519.

(40) Our previous studies[38] have shown that the chemistry of some of these macrocyclic ligand complexes can be complicated by complexation equilibria and the presence of different conformational isomers. In the present study we have adjusted halide concentrations to ensure maximum haloaquocobalt(III) species were present (as determined by NMR). The problem of isomers is a concern with complexes of the Me_6[14]4,11-dieneN$_4$ ligand, and some care must be exercised to ensure that the rates measured are for self-exchange reactions rather than for the reactions between different stereochemical iosmers of the oxidant and the reductant. This problem complicates the earlier studies of inner-sphere reactions with the $Co(Me_6[14]4,11\text{-dieneN}_4)(OH_2)^{2+}$ reductant[16a] since the procedures employed generate the *meso* isomer while the *rac* ligand isomer is usually the most stable from the $Co(Me_6[14]4,11\text{-dieneN}_4)(OH_2)X^{2+}$ complexes.[38] Of the present studies of $Co(Me_6[14]4,11\text{-dieneN}_4)(OH_2)X^{2+}$/$Co(Me_6[14]4,11\text{-dieneN}_4)(OH_2)^{2+}$ reactions, only for X = Cl did we determine an actual self-exchange rate constant.

$$Co(MCL)(H_2O)X^{2+} + Co(MCL^*)(H_2O)_2^{2+} \overset{K_o}{\rightleftharpoons} \{Co(MCL)(H_2O)X^{2+},Co(MCL^*)(H_2O)_2^{2+}\} \quad (3)$$

$$\{Co(MCL)(H_2O)X^{2+},Co(MCL^*)(H_2O)_2^{2+}\} \overset{k_w,K_w}{\rightleftharpoons} \{Co(MCL)(H_2O)X^{2+},Co(MCL^*)H_2O^{2+}\} + H_2O \quad (4)$$

$$\{Co(MCL)(H_2O)X^{2+},Co(MCL^*)H_2O^{2+}\} \overset{k_i,K_i}{\rightleftharpoons} \{H_2O(MCL)Co^{III}-X-Co^{II}(MCL^*)H_2O^{4+}\} \quad (5)$$

$$\{H_2O(MCL)Co^{III}-X-Co^{II}(MCL^*)H_2O^{4+}\} \overset{k_e}{\rightarrow} \{H_2O(MCL)Co^{II}-X-Co^{III}(MCL^*)OH_2^{4+}\} \quad (6)$$

longer than, the {A,B} lifetime. Equations 3−6 should be regarded as the simplest basis for analysis of the inner-sphere reaction pathway. Additional simplification is achieved if the usual[41] I_d mechanism for substitution on Co(II) is assumed, so that $k_i = K_o k_w$. The two chemically meaningful limits are as follows:[42] (a) substitution is rate limiting so that the overall rate constant is given by $k_{ab} = K_o k_w$; (b) electron transfer is rate limiting so that $k_{ab} = K_o K_w k_e$. Values of K_o are expected to be of the order of $10^{-0}-10^{-1}$ ($\mu = 1$), and k_w is approximately 10^8-10^9 s^{-1} for these low-spin complexes,[39,42] so k_{ab}(obsd) < $K_o k_w$ and the second limit is the most applicable to the self-exhange reactions.

In the weak-coupling limit, the electron transfer rate constant, k_e, can be formulated as in eq 7,[2,4-7] where κ_{el} is the electronic

$$k_e = \kappa_{el} \nu_{eff} \exp(-\Delta G^{\ddagger}/RT) \quad (7)$$

transmission coefficient, ν_{eff} is the effective frequency of nuclear motion near the transition state, $\Delta G^{\ddagger} = (\lambda/4)(1 + \Delta G°/\lambda)^2$, λ (the subscript "DA" has been dropped for simplicity) is the appropriate nuclear reorganizational parameter, and $\Delta G°$ is the free energy change in the electron transfer step.[2,4-14] In a self-exchange reaction $\Delta G^{\ddagger} = \lambda/4$. The nuclear reorganizational parameter is generally represented as a sum of molecular, λ_m, and solvent, λ_s, components (eq 8). If the electron transfer in

$$\lambda = \lambda_m + \lambda_s \quad (8)$$

eq 6 is accompanied by the countermotion of the bridging ligand, X^-, then the net change of charge is very small and $\lambda_s \cong 0$.[16]

In general, it is convenient to represent the changes in potential energy which accompany electron transfer in terms of the contributions which arise from the correlated displacements of nuclei from their equilibrium positions plus the

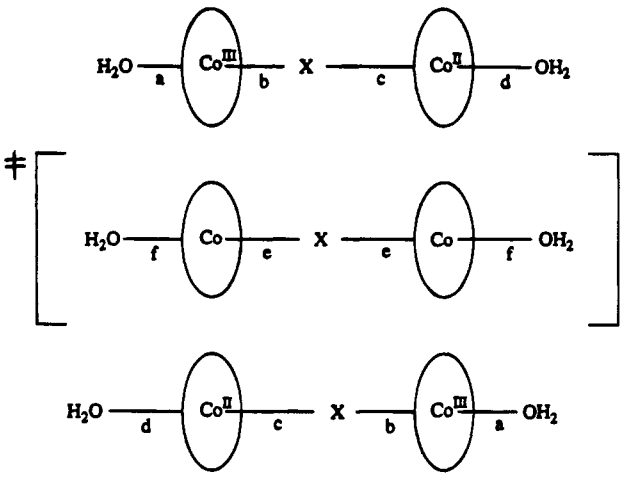

Figure 3. Scheme for description of "states" across the inner-sphere reaction coordinate.

contributions of the electronic energy of the system for each set of nuclear coordinates, typically as in eq 9 where the sum

$$PE = V = \sum_{i=1}^{n} {}^1/_2 f_i(x_i - x_i°)^2 + H_{DA}(x_1,x_2,...,x_n) \quad (9)$$

is over all nuclei, x_i is the displaced coordinate of the ith nucleus and $x_i°$ its equilibrium value, and the f_i are force constants. In the weak-coupling limit, such as is used in treatments of simple outer-sphere electron transfer,[2,4-14] $H_{DA} \gg 0$ and the contributions of the nuclear motions of the donor can be considered independently from those of the acceptor. This is not the case for the inner-sphere electron transfer reactions considered here. For example, Stritar and Taube[43] have pointed out that the bridging ligand motion involves a concerted expansion and compression of oxidant and reductant bond lengths in the inner-sphere reactions of dσ donors and acceptors. In order that such concerted motion can result in a smaller value of λ(IS) than of λ(OS), the electron transfer would have to occur in concert with the bridging ligand motion (see below). Thus, one can identify different sets of coordinates for the initial state, the transition state, and the final state as illustrated schematically in Figure 3. The concerted motion of the electron and the bridging ligand (X in Figure 3) between metal centers implies that the work done stretching the $Co^{III}-X$ bond (a repulsive potential term) is partly compensated by an attractive interaction of X with the other metal center; alternatively, if the electron density were not redistributed rapidly on the time scale for this nuclear motion, then the $Co^{II}-X$ compression would be repulsive. For the *trans*-$Co(MCL)(OH_2)_2X^{2+}/Co(MCL)(OH_2)_2^{2+}$ couples considered here, the equatorial Co−N bond lengths are nearly identical in both oxidation states, so it is convenient to use a single coordinate (i.e., along the Co−X−Co axis), **x**.

This simple linear coordinate for the inner-sphere reaction pathway suggests that at least some of the lowered activation energy characteristic of the inner-sphere pathway for σ-donor and σ-acceptor systems derives from the smaller net bond length changes which result when the expansion of the $Co(III)-Cl^-$ bond occurs in concert with compression of the Cl^-−Co(III) bond. In the simplest limit, when $c \cong d$ and $a \cong b$ in Figure 3, and assuming the potential energy functions are second order in the nuclear displacements, the net displacement for this inner-sphere pathway is about 75% that for the corresponding outer-sphere reaction so that $\lambda_m(IS) \cong 0.6\lambda_m(OS)$. This is surprisingly

(41) Wilkins, R. D. *The Study of Kinetics and Mechanisms of Reactions of Transition Metal Complexes*; Allyn and Bacon: Boston, 1974.

(42) (a) Variations in K_o are expected to be small and have been discussed elsewhere.[21] The approach described here does not allow for any variations in precursor complex stabilities (K_i). This corresponds to the choice of an initial state, in the perturbational argument, in which there is no donor−acceptor or vibronic coupling. Variations in stereochemical repulsions could lead to variations in the Co−X−Co distance, but this would appear in λ(IS). Variations in K_w probably parallel variations in k_w, and k_w is larger for $Co(Me_6[14]dieneN_4)(H_2O)_2^{2+}$ than for $Co(Me_4[14]tetraeneN_4)(H_2O)_2^{2+}$,[39,42b,c] possibly increasing the range of actual values of k_e inferred from k_{exch}. If vibronic coupling results in a lower ground state energy than that associated with the $\{Co(MCL)(H_2O)X^{2+},Co(MCL)H_2O^{2+}\}$ species, then K_i would be a factor and $k_{ab} = K_o K_w K_i k_e$. This is likely only when LMCT mixing is very strong, i.e., when $|\beta_o| \gg \lambda_i$(IS), Δ. (b) Tait, A. M.; Hoffman, M. Z.; Hayon, E. *J. Am. Chem. Soc.* **1976**, *98*, 86. (c) Durham, B. Ph.D. Dissertation, Wayne State University, 1978.

(43) Stritar, J.; Taube, H. *Inorg. Chem.* **1969**, *8*, 2281.

close to the experimental inference[16] that $\lambda_m(IS) \cong 0.5\lambda_m(OS)$. That such an oversimplified argument should be even roughly correct suggests that some features of the usual models for weakly coupled electron transfer systems are retained in at least some inner-sphere systems. Of course, one needs a more detailed treatment to account for the observed bridging ligand dependencies of the reaction rates, and one needs to explicitly take account of a simultaneous redistribution of electron density with nuclear motion.

A simple model of the inner-sphere electron transfer reaction coordinate can be premised on the major points summarized above: (1) the bridging ligand dependence of the reaction rates probably has much of its origin in non-reorganizational factors, (2) the values of $\lambda_m(IS)$ are intrinsically smaller than those of $\lambda_m(OS)$, and (3) the bridging (and other correlated) ligand motion is coupled to the redistribution of electron density. These issues are actually interrelated through the effects of different distributions of electron density. In order to develop a simple model of the reaction coordinate, we will initially develop a model for a "purely electronic" contribution of the bridging ligand, and then we will integrate this model into a vibronic coupling model of the reaction coordinate.

For our purposes it is useful to initially consider the consequences of a symmetrically bridged system (X centered between the metals). The bridging ligand p_z orbital and the metal d_{z^2} orbitals can be combined in a 3-center, 3-electron bond, since the electron affinity of Cl (and most "good" bridging ligands) is so much greater than that of Co(III), the 3-center interaction is best treated in terms of perturbational mixing of a {Co(II), •Cl, Co(II)} excited state configuration (with associated wave function Ψ_c) with symmetry-adapted combinations of reactants, {Co(III)−Cl⁻, Co(II)}, and products, {Co(II), Cl⁻−Co(III)}. The net result will be a charge transfer stabilization of one component of the symmetry-adapted reactant and product species. If we use a wave function Φ_R to designate the reactants and Φ_P to designate the products, then the appropriate symmetry-adapted functions are given by eqs 10a,b. The Ψ_a function

$$\Psi_s = \frac{1}{\sqrt{2}}(\Phi_R + \Phi_P) \tag{10a}$$

$$\Psi_a = \frac{1}{\sqrt{2}}(\Phi_R - \Phi_P) \tag{10b}$$

correlates with a 3-center bonding interaction utilizing the p_z orbital of X, and this can be used to model the transition state. In the absence of any direct Co/Co coupling, the energy of this state, $E_a^\circ = \langle\Psi_a|H|\Psi_a\rangle$, will be lowered through mixing with the {Co(II), •X, Co(II)} configuration. This amounts to a charge transfer stabilization[44] of the transition state as schematically illustrated in Figure 4. The stabilization energy, as given by first-order perturbation theory,[43] will be as in eq 11, where β_{CT}

$$\epsilon_{CT}^\circ \cong \beta_{CT}^2/E_{CT} \tag{11}$$

$= H_{ac} - SE_a^\circ$, S is an overlap integral, and $H_{ac} = \langle\Psi_a|H|\Psi_c\rangle$. Since ϵ_{CT}° is the resulting energy of stabilization of the symmetry-adapted transition state, it will be appreciably smaller than the analogous LMCT stabilization energy of the Co(MCL)-$(OH_2)Cl^{2+}$ reactant ground state but larger that that of an isolated $Co(MCL)(OH_2)Cl^{2+}$ molecule with bond lengths adjusted to those of the transition state. When no other factors are varied, values of ϵ_{CT}° will vary approximately with the inverse of the ionization energy of X^- and will approximately correlate with LMCT energies of the $Co(MCL)(OH_2)X^{2+}$ ground state. The effect of the LMCT mixing is to delocalize some electron density along the 3-center axis and thus provide a mechanism for electronic coupling between the donor and acceptor.

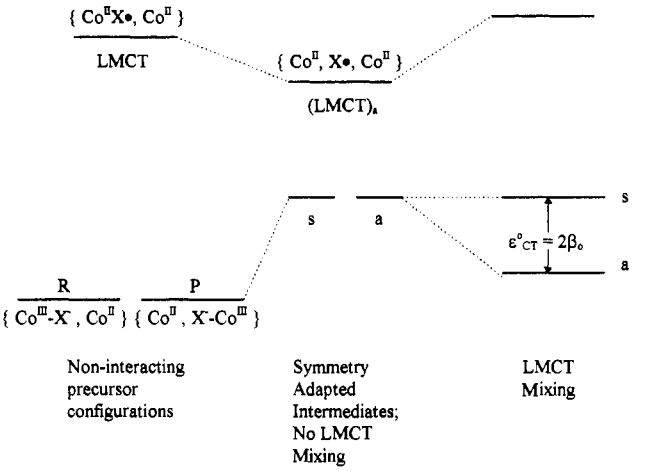

Figure 4. Qualtitative scheme illustrating the mixing of electronic wave functions in a halide-bridged (p_z) symmetrical inner-sphere (σ, d_{z^2}) electron transfer system.

The coupled nuclear and electronic motion which seems intrinsic to this problem means that the Born−Oppenheimer approximation, which is assumed in most outer-sphere electron transfer treatments,[2,4-14] is not valid. A vibronic approach can often give useful results in such situations[45-47] and has been used to treat the spectra of some classes of bridged donor−acceptor complexes.[48] Since we have postulated that LMCT coupling results in an intrinsic difference in the energies of the symmetry-adapted transition state electronic configurations, the problem considered here is analogous to a pseudo-Jahn−Teller problem.[46] If we postulate that the coupling between the metal centers decreases as their separation increases, $\beta_{sa} \cong \beta_o + ax_r$, and if we introduce the coupling perturbations in succession so that $\epsilon_{CT}^\circ = 2\beta_o$, then eqs 12a,b define the appropriate potential

$$V_s \cong V^\circ + \beta_o + kx_r^2/2 \tag{12a}$$

$$V_a \cong V^\circ - \beta_o + kx_r^2/2 \tag{12b}$$

energy functions where x_r is the reaction coordinate discussed above and k is a force constant. The roots of the corresponding secular eq are given by eqs 13 and 14. Of these, V_- represents

$$V_+ = V^\circ + kx_r^2/2 + [\beta_o^2 + (ax_r)^2]^{1/2} \tag{13}$$

$$V_- = V^\circ + kx_r^2/2 - [\beta_o^2 + (ax_r)^2]^{1/2} \tag{14}$$

the lower surface (i.e., the reaction coordinate). Two limits can be distinguished:[46] (a) $\beta_o^2 \gg a^2x_r^2$, corresponding to a single PE minimum and occurring when LMCT energies are relatively low (easily oxidized bridiging ligand, X^-); (b) $\beta_o^2 << a^2x_r^2$, in which case there are two PE minima corresponding to the conventional picture of electron transfer reactants and products.

(44) Mulliken, R. S.; Person, W. B. *Molecular Complexes*; Wiley-Interscience: New York, 1969.
(45) Ballhausen, C. J. In *Vibronic Processes in Inorganic Chemistry*; Flint, C. D., Ed.; Kluwer: Dordrecht, 1988, p 33.
(46) Bersuker, I. B. *The Jahn-Teller Effect and Vibronic Interactions in Modern Chemistry*; Plenum: New York, 1984; pp 61−69.
(47) Fischer, G. *Vibronic Coupling*; Academic: New York, 1989.
(48) Piepho, S. B. *J. Am. Chem. Soc.* **1990**, *112*, 4197.
(49) Schläfer, H. L.; Glieman, G. *Ligand Field Theory*; Wiley: New York; 1969.

Before we consider the activation energy implied by eq 14, it is useful to consider the weakly coupled limit, $\beta_o = 0$, for this model. In this limit, the PE minima occur at $(x_r)_{min} = \pm a/k$, $(V_-)_{min} = V^\circ - a^2/2k$, and for the same set of nuclear coordinates ($x_r = a/k$) $(V_+)_{a/k} = V_o + 3a^2/2k$. In this weak-coupling limit the usual electron transfer logic should prevail and one expects that $(V_+ - V_-)_{a/k} = \lambda(IS)$, so that $a \cong [k\lambda(IS)/2]^{1/2}$. Provided β_o is sufficiently small, this parametrization will work well in eq 14 leading to eq 15. On the basis of these

$$(V_-)_{min} \cong V^\circ + \lambda(IS)/4 - [\beta_o^2 + \lambda(IS)^2/4]^{1/2} \cong V^\circ - \lambda(IS)/4 - \beta_o^2/\lambda(IS) \quad (15)$$

arguments, one expects a double minimum for the inner-sphere electron transfer PE surface only when the nuclear reorganizational energy is large and when LMCT transitions occur at high energy. Equations 14 (with $x_r = 0$) and 15 allow us to express the inner-sphere activation energy as in eq 16. The $\beta_o^2/\lambda(IS)$

$$\Delta V^\ddagger \cong \lambda(IS)/4 + \beta_o^2/\lambda(IS) - \beta_o \quad (16)$$

term in eqs 15 and 16 corresponds to the expected first order perturbational stabilization of the ground state which arises from mixing with the electron transfer excited state.[44] This mixing results in a residual barrier to electron transfer even when $\lambda(IS)/2 \cong \epsilon_{CT}^\circ$.

The experimental observations are qualitatively in accord with eq 15 since (1) there does seem to be some contribution of nuclear reorganizational energy to the rate patterns (Tables 2 and 3) and (2) k_{exch} tends to increase when E_{CT} decreases (corresponding to increases in β_o). It is difficult to estimate how large the effects should be. If we estimate $\epsilon_{CT}^\circ \sim E_{CT}/4 \sim 1 \times 10^3$ cm^{-1} and $\lambda(IS)/4 \sim 2 \times 10^3$ cm^{-1} for X = Cl, then a ~20% change in both β_o and $\lambda(IS)/4$ when X is changed to Br would be required to give the approximately 10-fold increase observed in k_{exch}. The structural perturbations of the MCL ligands have little effect on k_{exch} for the azide-bridged reactions. This would suggest smaller contributions to $\lambda(IS)$ from Co−ligand bond length changes, perhaps compensated by bond length changes within the azide bridge.[50]

In the Introduction we noted that the physical meaning of the self-exchange reorganizational energies inferred from cross-reaction data is not obvious for inner-sphere reactions. The vibronic model proposed above can be used to address this point. To do so, it is convenient to define the potential energy functions, as in eqs 17a,b where Δ is the energy difference

$$V_R = kx_r^2/2 - \beta_o \quad (17a)$$

$$V_P = \Delta + kx_r^2/2 + \beta_o \quad (17b)$$

between the two electron transfer states for the coordinates of the preassociated reactant complexes. Proceeding as before, we obtain solutions of the secular determinant as in eq 18. After

$$V_\pm \cong \Delta/2 + kx_r^2/2 \pm [\Delta^2 + 4\beta_o^2 + \lambda 4a^2x_r^2]^{1/2}/2 \quad (18)$$

minimizing V_- with respect to x_r and using the parametrization described above, this model leads to eq 19 as an approximate description of the reaction coordinate (assuming Δ^2 and β_o^2 are

$$V_- \cong \Delta/2 + \lambda(IS)^*/4 - [\Delta^2 + 4\beta_o^2 + \lambda(IS)^{*2}]^{1/2}/2 \quad (19)$$

small; we have used the asterisk to designate the reorganizational parameter for an unsymmetrical reaction; see the following discussion). In the limit that $\beta_o \cong 0$ and $\Delta^2 \ll \lambda(IS)$, eq 19 reduces to eq 20. We can take V_R evaluated at $x_r = 0$ as a

$$V_- \cong \Delta/2 - \lambda(IS)^*/4 - \Delta^2/(4\lambda(IS)^*) \quad (20)$$

definition of the PE for the transition state for electron transfer, so that the activation energy for electron transfer in this limit is $\Delta V^\ddagger \cong -V_-$. This is exactly the usual result for weakly coupled electron transfer systems.[2,4-14] The extraction of $\lambda(IS)^*$ parameters from experimental data should be straightforward in this regime (i.e., for small equilibrium constant magnitudes).

When $\Delta^2 \gg 4a^2x_r^2$, eq 17 does not have a unique minimum, and $\Delta V^\ddagger$ approaches a constant value in this regime;[51] i.e., when $\Delta^2 > \lambda(IS)^{*2}$, the rates of the corresponding inner-sphere electron transfer reactions should become very nearly independent of the free energy of reaction and the reorganizational parameters. This is in reasonable agreement with earlier observations on this class of reactions.[16] It would be impossible to extract useful information about $\lambda(IS)^*$ from kinetic data obtained in this regime.

It is of interest that the driving force dependence implied by eqs 17a,b is essentially identical to that of the well-known Rehm−Weller eq.[52] It seems likely that the Rehm−Weller eq is in principle applicable to electron transfer systems in which nuclear and electronic motions are strongly coupled. To our knowledge, this had not been noted previously.

The vibronic model described above treats the concerted motion of the bridging ligand in a manner which is somewhat equivalent to the asymmetric stretching motion of a linear triatomic molecule. From such a point of view, the amplitude of the "bridging ligand motion" is not always a well-defined concept; rather, all the correlated atoms must move to an extent which is weighted by relative masses. Since the amplitudes of the net nuclear motions will depend on the atomic mass ratios, one expects that $\lambda(IS)$ must also be a function of the masses of the bridging atom and the atoms bridged. The issue can be readily addressed in the triatomic limit (see the Appendix).

In order to properly assess the effect of the concerted bridging ligand motion on $\lambda(IS)$, the individual nuclear displacements must be evaluated in the center of mass coordinates. For a "symmetrical" system, appropriate to a self-exchange reaction, all three nuclei must move with respect to the center of mass in response to electron transfer. The resulting expression for $\lambda(IS)$, eq 21 (in which $\lambda^\circ(IS)$ is the reorganizational energy based

$$\lambda(IS) = [k(c-b)^2/2][2(2+\mu^2)/(2+\mu)^2] = [\lambda^\circ(IS)]g \quad (21)$$

only on bond length differences (defined as in Figure 3), g is a mass-dependent correction term ($g = 1$ for $\mu = 0$; $g = 2$ for $\mu = \infty$), and μ is the ratio of the mass of the bridging ligand to that of Co), predicts a fairly shallow dependence of the self-exchange rate constant on the mass of the bridging ligand: (a) for $0 \le \mu \le 2$, $\lambda(IS)$ decreases 33%; (b) for $\mu > 1$, it increases monotonically to a maximum value of 2. For both X = Cl and X = Br, $\lambda(IS) \cong 0.7\lambda^\circ(IS)$, so none of the *variations* in k_{exch} observed here can be ascribed to a simple mass effect. However, these relatively massive bridging ligands may give rise to observed values of k_{exch} which are about an order of

(50) Donor−acceptor coupling which is mediated by π-ligands seems to involve significant nuclear motion within the ligand.[22] The azide bridging ligand coupling of $d\sigma/d\sigma$ D/A systems could be complicated by electronic factors since $d\sigma/d\pi$ mixing of nearest neighbors may be weak. If this were the case here, κ_{el} would be much smaller for the N_3 than for halide bridging ligands.

(51) A value of $\Delta V^\ddagger \cong \beta_o^2\lambda(IS)^*/\Delta^2$ can be obtained if the matrix element is defined as $\beta_{RP} = \beta_o + ax_r$, $V_R \cong kx_r^2/2$ and $V_P \cong \Delta + kx_r^2/2$.

(52) Rehm, D.; Weller, A. *Isr. J. Chem.* **1970**, *8*, 259.

magnitude larger than would be expected on the basis of bond length changes only (i.e., $\lambda°(IS)$).

In this greatly simplified limit, the reorganizational energy for an inner-sphere cross-reaction is given by eq 22 in which p

$$\lambda(IS)_{AB} \cong g\lambda°(IS)_{AA}\left[1 + p + \frac{2 + (1+\mu)^2}{2(2+\mu^2)}p^2\right] \quad (22)$$

$= \partial/(c - b)$, AA represents the component self-exchange couple with the smallest axial bond length change ($c - b$), and $\partial = (c' - c)$ is the difference in Co(II) axial bond lengths in the two component (AA and BB) couples. The average of the reorganizational energies of the component couples, $\lambda(IS)^{av}_{AB}$, is often used as an estimate of $\lambda(IS)_{AB}$, but in the present kind of system this could lead to appreciable errors. Since $\lambda(IS)^{av}_{AB}$, can be represented as in eq 23 and since values of p are expected

$$\lambda(IS)^{av}_{AB} = [\lambda(IS)_{AA} + \lambda(IS)_{BB}]/2$$
$$\cong g\lambda°(IS)_{AA}[(1+p)^2 + 1]/2 \quad (23)$$

(on the basis of $Co(MCL)(OH_2)_2^{2+}$ crystal structures[21,53]) to have a maximum value of about $^1/_3$ for the compounds employed here, one expects that $\lambda(IS)_{AB} \leq 1.08\lambda(IS)^{av}_{AB}$. Thus, the coupled motions of donor, acceptor, and bridging ligand atoms are likely to lead to substantial systematic errors in cross-reaction data when the reaction systems involve large bond length changes and when eq 23 is used for the types of inner-sphere electron transfer processes described here.

These deviations from eq 23 may complicate the detailed interpretation of the previously observed correlation between $\lambda(IS)$ and $\lambda(OS)$,[16a] but the preceding argument does not alter our inference that $\lambda(IS) < \lambda(OS)$. However, the simple model discussed above does suggest that some of the differences in these reorganizational parameters may arise from the different reduced masses for the respective concerted (inner-sphere limit) and independent (outer-sphere limit) nuclear motions.

Conclusions

NMR line-broadening experiments have substantiated earlier inferences (based on cross-reactions) that in some halide-bridged, self-exchange electron transfer reactions of low-spin *trans*-$Co(MCL)(OH_2)Cl^{2+}/Co(MCL)(OH_2)^{2+}$ couples (1) the inner-sphere self-exchange rates are about 10^6 times faster than their outer-sphere equivalents, (2) rate patterns are a function of nuclear reorganizational energies, and (3) the nuclear reorganizational energy appropriate for the Cl^--bridged pathway among these complexes is about half that of the analogous outer-sphere reaction pathway. The observations strongly suggest that bridging ligand motion and electron transfer are coupled in these systems, so that Born–Oppenheimer-based theoretical models would not provide appropriate descriptions of the reaction coordinate. A simple vibronic approach is developed which does have many features that are consistent with the observations. The model contains the following features: (1) an intrinsic donor–acceptor coupling, β_o, which can be described in terms of ligand-to-metal charge transfer stabilization of the transition state; (2) donor–acceptor coupling which varies with the position of the bridging ligand (more correctly, the donor–acceptor coupling varies with the position along the reaction coordinate); (3) a variation in rate with the bridging ligand much of which is attributable to variations in LMCT stabilization energies, and some results from the effect of mass of the bridging ligand on the dynamics of the concerted nuclear motion. Several limiting cases have been considered, and the vibronic model maps into the usual Marcus–Hush-type electron transfer expressions when $\beta o \sim 0$ (weak donor–acceptor coupling), except when electron transfer invovles a very large driving force. In this limit the vibronic model predicts that observed rates should approach a limiting value, as opposed to Marcus-type inverted-region behavior, and this is consistent with the limited information available from earlier work (rate constants independent of $\Delta G°$ over about a 1 eV range).[16] There are some potential problems in the interpretation of inner-sphere reorganizational energy in the cross-reactions due to the effect of bridging ligand mass on the coupled nuclear motions.

Acknowledgment. We are grateful to the donors of the Petroleum Research Fund, administered by the American Chemical Society, and to the Fundamental Interactions Branch, Division of Chemical Sciences, Office of Energy Sciences, Department of Energy, for partial support of this research. C.L.S. gratefully acknowledges partial support through a Graduate and Professional Opportunities Scholarship from the Department of Education.

Appendix

For simplicity we consider a linear three-particle system, e.g., with x_1 the coordinate of Co(III), x_2 the coordinate of the bridging ligand, and x_3 the coordinate of Co(II). The center of mass coordinates are based on the set of boundary conditions in eqs 24a–c, where the last

$$-x_1 + x_2 = b \quad (24a)$$

$$-x_2 + x_3 = c \quad (24b)$$

$$\mu x_2 + x_3 + x_1 = 0 \quad (24c)$$

of these eqs is obtained by integrating the corresponding linear momentum conservation eq. Simultaneous solution of these eqs gives eqs 25a–c for the x_i. The coordinates after electron transfer are

$$x_1 = [c + (1+\mu)b]/(\mu + 2) \quad (25a)$$

$$x_2 = (c - b)/(\mu + 2) \quad (25b)$$

$$x_3 = [b + (1+\mu)c](\mu + 2) \quad (25c)$$

obtained by interchanging b and c in these eqs. Since $\lambda(IS)_{AA} = (k/2)\sum_i(\Delta x_i)^2$, the result in eq 21 follows after some algebraic manipulation. For a cross-reaction in which the reactant and product Co(II) complexes have axial bond lengths which differ by ∂, we similarly obtain eqs 26a–c for the $\Delta x_i'$, and eq 22 is the result.

$$\Delta x_1' = -\mu(c - b)/(\mu + 2) - \delta(1+\mu)/(\mu + 2) \quad (26a)$$

$$\Delta x_2' = 2(c - b)/(\mu + 2) + \delta/(\mu + 2) \quad (26b)$$

$$\Delta x_3' = (c - b)\mu/(\mu + 2) - \delta/(\mu + 2) \quad (26c)$$

IC950226G

(53) Endicott, J. F.; Lilie, J.; Kuszaj, J. M.; Ramaswamy, B. S.; Schmousees, W. G.; Simic, M. G.; Glick, M. D.; Rillema, D. P. *J. Am. Chem. Soc.* **1977**, *99*, 429.